Fluorophosphonates on-Demand: A General and Simplified Approach toward Fluorophosphonate Synthesis

Jason K. Dutra,*[a] Timothy L. Foley,[a] Zhen Huang,[b] Ethan L. Fisher,[a] Erik A. Lachapelle,[a] Subham Mahapatra,[a] Kevin Ogilvie,[a] Todd W. Butler,[a] Justin Bellenger,[a] Jaimeen Devraj Majmudar,[b] and Christopher W. am Ende[a]

Herein, we report a general and simplified synthesis of fluorophosphonates directly from *p*-nitrophenylphosphonates. This FP on-demand reaction is mediated by a commercially available polymer-supported fluoride reagent that produces a variety (25 examples) of fluorophosphonates in high yields while only requiring reagent filtration for pure fluorophosphonate isolation. This reaction protocol facilitates the rapid profiling of serine hydrolases with diverse and novel sets of activated phosphonates with differential proteome reactivity. Moreover, slight modification of the procedure into a reaction-to-assay format has enabled additional screening efficiency.

Serine hydrolases (SHs) are a superfamily of enzymes that catalyze the hydrolysis of amide, ester, and thioester bonds via a catalytic diad or triad mechanism, whereby a histidine and/or aspartate act as a base to enhance the nucleophilicity of the active site serine residue.[1] Given their diverse nature, SHs play crucial roles in many biological pathways,[2] and thus, have generated significant interest as potential pharmaceutical targets.[3] The development of activity-based probes (ABPs) that engage the SH family of enzymes have helped identify and elucidate the functions of SH targets, including their roles in cellular differentiation and have shown immense value in the development of selective SH inhibitors.[2a,4] Although a variety of reactive functional groups have been employed to covalently modify SHs,[1c,5] activated phosphonate warheads, including fluorophosphonates (FPs)[6] and *p*-nitrophenylphosphonates (*p*NPs),[7] have been amongst the most utilized as ABPs (Figure 1A). Additionally, comparative analyses of activated phosphonates of differing chemotypes[8] highlight the benefits of having access to a toolbox of probes with readily tunable reactivity[8b,9] for labeling SHs. All these examples serve to highlight that structurally diverse probes are of immense value to better understand SH roles in various biological contexts.

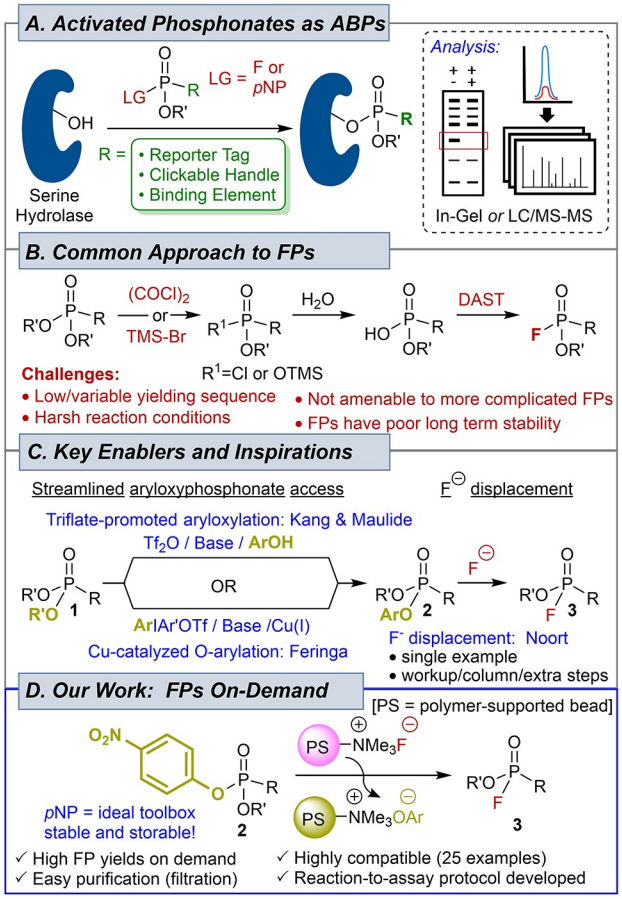

Figure 1. Common uses and synthesis of activated phosphonates.

Access to diversified FPs has been hampered by their limited commercial availability, coupled with challenging syntheses that often proceed in low or highly variable yields.[6a,10] FPs are typically accessed by converting dialkyl phosphonates to highly reactive and labile phosphonochloridate or silyloxyphosphonate intermediates, which are then hydrolyzed and finally treated with a dehydrating fluorination reagent (e.g., DAST)[11] to generate the desired FP (Figure 1B). The low functional group tolerance to the harsh reaction conditions limit access to more complicated FPs through this chemistry. Moreover, isolation and purification of FPs derived from this approach often requires aqueous workup, chromatography,

[a] J. K. Dutra, Dr. T. L. Foley, Dr. E. L. Fisher, E. A. Lachapelle, Dr. S. Mahapatra, K. Ogilvie, T. W. Butler, J. Bellenger, Dr. C. W. am Ende
Pfizer Worldwide Research and Development
Eastern Point Road, Groton, CT 06340 (USA)
E-mail: jason.k.dutra@pfizer.com
[b] Dr. Z. Huang, Dr. J. Devraj Majmudar
Pfizer Worldwide Research and Development
1 Portland St, Cambridge, MA 02139 (USA)

Supporting information for this article is available on the WWW under https://doi.org/10.1002/cbic.202000852

This article is part of a Special Collection on Chemical Translational Biology. Please see our homepage for more articles in the collection.

and/or distillation, which can contribute to product degradation and yield reduction. Finally, the isolated FPs must be used immediately or stored under dry or cryogenic conditions to prevent degradation due to their reactive nature and lability to hydrolysis over time.[6g]

To address many of these issues, we set out to develop a new FP synthesis on-demand protocol, whereby *p*NPs are rapidly converted, in a single, final step, to their FP counterparts. The overarching strategy uses *p*NPs as the key components of a multi-purpose "phosphonate toolbox" by leveraging *p*NPs innate reactivity and traditional role as covalent SH inhibitors and ABPs,[7] while also exploiting the *p*NPs as flexible late-stage synthetic intermediates. An ideal chemical toolbox should be easily storable to facilitate use as needed. We have observed that *p*NPs are highly stable, and thus more amenable to longer term storage, when compared to their corresponding FPs, which degrade over time under comparable storage conditions (Table 1 and Section 3 in the Supporting Information).

Analysis of the literature shows that *p*NPs have flexibility as late-stage synthetic intermediates, with examples of amidation,[12] carbamate formation,[7b–d,13] click chemistry,[7d,12b,14] and alkylation[15] in the presence of an electrophilic *p*NP group. Moreover, the use of nucleophilic fluoride ion can be a powerful and simple approach to affect leaving group modification on a variety of electrophilic organophosphorus centers.[6g,15,16] For example, Townsend et al.[6g] recently demonstrated a new approach to form the phosphorus-fluorine bond of a functionally complex FP by displacing the phenoxide of a diphenylphosphonate with fluoride ion. This method, however, required a subsequent O-methylation step using diazomethane[17] to ultimately prepare the FP. Fluoride displacement of nitrophenoxide leaving groups on mixed phosphonates has also been reported in kinetic studies[16a,c] or as an unintended side reaction,[16f] but none of these examples demonstrate the isolation of FP products. Noort and co-workers[16g] further inspired us by demonstrating a single example of *p*NP displacement with a solution phase fluoride ion source to synthesize a FP in 90% isolated yield (Figure 1C). However, their procedure required chromatography and additional deprotection and condensation steps to complete the synthesis.

The ability to rapidly synthesize a diverse array of *p*NPs for toolbox preparation is necessary to enable this strategy. We chose to use the recently developed, and mechanistically diverse, triflate-mediated phosphonate aryloxation[18] and copper-catalyzed iodonium phosphonate aryloxation methodologies[19] which enable rapid and simplified synthetic access to mixed aryloxyphosphonates (including *p*NPs) directly from dialkylphosphonates in a single step (Figure 1C, see Section 2.3 in the Supporting Information for details, yields ranged from 69–100%). It is noteworthy that Kang's method[18a] also worked well when applied to several alkyne-bearing dialkylphosphonates, which are highly desirable for compounds that can be used in SH activity-based protein profiling (ABPP) experiments.

With the preceding information, and a variety of *p*NP precursors in hand, we set out to develop a general fluoride-mediated *p*NP→FP reaction protocol. Our reaction design criteria included utilization of a commercially available fluoride source, mild conditions with broad substrate compatibility, and overall operational simplicity with minimal purification and handling required to isolate pure FP products in high yields. We envisioned that a polymer-supported fluoride exchange reagent[20] could enable many of these objectives, In principle, it should deliver nucleophilic fluoride anion to displace the *p*-nitrophenol leaving group, and subsequent filtration of the insoluble polymer-supported reagent, which captures the phenolic leaving group, would yield pure FP in solution (Figure 1D).

After reducing the reaction design criteria to practice, our FP on-demand protocol (see the Experimental Section and Section 2.4 in the Supporting Information for details) enabled the conversion of 25 *p*NPs (**2**) into the corresponding pure FPs (**3**) in high isolated yields (80–100%; Scheme 1). Linear aliphatic (**3a**–**k**), aromatic (**3n**–**t**), and polar substrates bearing heterocycles (**3u**–**x**) and PEG units (**3l, 3w**–**x**) performed well, as did phosphonates with increased steric hinderance near the reactive phosphorus center (**3m, 3r**). We recently described the solution phase preparation of **3w**–**x**[15] by displacing their corresponding *p*NPs (**2w**–**x**) with a TBAF•-(*tert*-BuOH)$_4$ complex in 62 and 71% chromatographic yields, respectively. However, using our new FP on-demand protocol to synthesize **3w**–**x**, we significantly improved yields to 90 and 95%, respectively, with greater operational ease.

We next evaluated the effects of the electronic characteristics of the aryloxy leaving group on the course of the reaction (Table 2). Mixed aryloxyphosphonates with electron-poor leaving groups (entries 1–3) all produce FP **3t** in high yields, with no modifications to the general procedure. However, starting materials with electron rich leaving groups result in incomplete conversion, despite longer reaction times (entries 4, 5, and 8) or elevated temperatures (45 °C, entries 6 and 9). Product decomposition was observed with significant increases in reaction time (entry 7) and temperature (85 °C, entry 10).

Table 1. Stability of *p*-nitrophenylphosphonates versus fluorophosphonates.

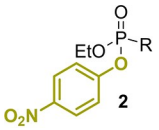

2a/3a: R = $(CH_2)_3C{\equiv}CH$
2c/3c: R = $(CH_2)_{14}C{\equiv}CH$
2f/3f: R = $(CH_2)_{14}CH_3$

Compound[a]	Storage time	Storage temp.	% Degradation[a]
2a	22 months	−20→4 °C[b]	0%
3a	22 months	−20→4 °C[b]	100%
2c	5 months	25 °C	0%
3c	5 months	25 °C	77%
2f	8 months	−20 °C	0%
3f	4.5 months	−20 °C	18%

[a] Determined by ^{31}P NMR (see Section 3 in the Supporting Information). [b] Stored at −20 °C for 17.5 months, then at 4 °C for 4.5 months (22 months total).

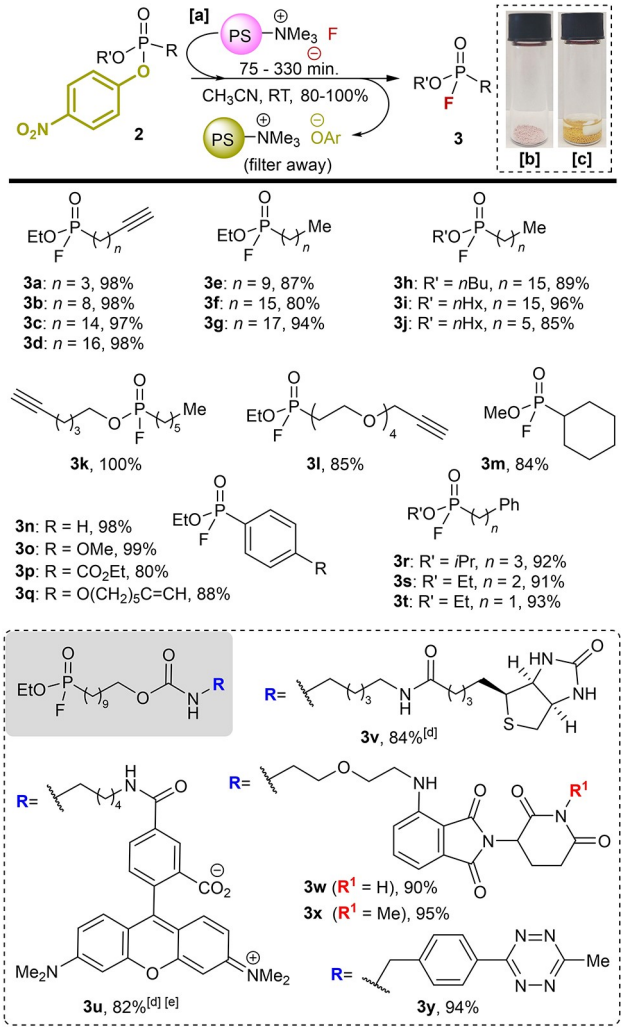

Scheme 1. Synthesis of fluorophosphonates according to the FP on-demand protocol. Conditions: 21–325 μmol **2**, 1.5–4.0 equiv. of fluoride on polymer support reagent, 0.08–0.15 M CH_3CN. [a] PS = polymer support. [b] The polymer-supported fluoride reagent is pink in color prior to *p*NP (**2**) addition. [c] The color of the polymer-supported reagent changes to yellow as it captures the *p*-nitrophenoxide leaving group. [d] CH_2Cl_2 was used as the solvent. [e] Pale pink→yellow color change was not observed due to the dark purple color of the TAMRA dye. [f] 7.2 equiv. of fluoride on polymer support reagent was used.

Table 2. Leaving group tolerance for the FP on-demand protocol.

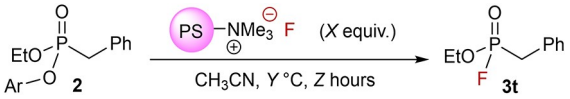

	2 (Ar)	X/Y/Z	Conv.[a]	Yield[b] 3t
1	**2t** (p-$NO_2C_6H_4$)	2.0/25/3 3.0	100%	93%[c]
2	**2y** (o-$NO_2C_6H_4$)	2.0/25/3	100%	100%
3	**2z** (C_6F_5)	1.5/25/2.5	100%	89%
4	**2aa** (C_6H_5)	2.0/25/8	25%	–
5	**2aa** (C_6H_5)	2.0/25/72	50%	–
6	**2aa** (C_6H_5)	2.0/45/24	55%	–
7	**2aa** (C_6H_5)	2.0[d]/45/96	decomp.	–
8	**2ab** (p-$MeOC_6H_4$)	1.5/25/2.5	0%	–
9	**2ab** (p-$MeOC_6H_4$)	1.5/45/16	20%	–
10	**2ab** (p-$MeOC_6H_4$)	1.5/85/24	decomp.	–

Reactions were performed on a 100–325 μmol scale. [a] Reaction conversion monitored and determined by ^{31}P NMR. [b] Yield of pure, isolated product. [c] From Scheme 1. [d] After 24 h, additional polymer-supported fluoride reagent (2.0 equiv) was added (4.0 equiv. total) then stirred at 45 °C for an additional 72 h (96 h total).

To further exemplify the utility of the "phosphonate toolbox" and our FP on-demand methodology, we assessed the reactivity of a diverse set of *p*NPs and FPs in differentiated human adipose-derived stem cells (hASCs) using in-gel ABPP coupled with Cu^I-catalyzed 1,3, dipolar Hüisgen cycloaddition ("click chemistry") with TAMRA-azide.[21] Adipocytes have a fundamental role in lipid metabolism and contain a large number of serine hydrolases, making them well suited for evaluating probe reactivity with this enzyme class. Live differentiated human adipocyte stem cells were treated with 1 and 10 mM *p*NP or FP probes for 1 h, after which the cells were washed with PBS, lysed, subjected to Cu^I-catalyzed azide–alkyne cycloaddition with 5-TAMRA-azide, and the labeled proteins were resolved by SDS-PAGE and visualized with in-gel fluorescence (Figure 2). The data showed protein labeling, many of which are presumed to be serine hydrolases. Compared to HDFP-alk (**3d**),[6e] shorter chain FP-alkyne probes (**3a–c**) labeled additional proteins. Compared to linear probes, the branched-chain probe (**3k**) labeled only a subset of proteins targets, which may prefer branched-chain lipid substrates. The *p*NP probes showed lower reactivity with the proteome, labeling a smaller set of proteins when compared to their FP analogs. Taken together, the panel of FP and *p*NP ABPs showcase the need for a diverse set of probes, as the structure of the probe can greatly influence the proteome reactivity.

Next, we sought to further streamline our process by adapting our FP on-demand procedure into a *reaction-to-assay* protocol, whereby pure FPs can be generated from *p*NPs in an assay-ready solvent (i.e., DMSO), while using equipment and consumable supplies commonly found within biological laboratories. Toward this end, we modified the existing procedure (see Section 5.1 in the Supporting Information) by executing the reaction at lower concentration (5 mM of *p*NP-rhodamine **2u** in [D_6]DMSO in the presence of excess polymer supported fluoride) in an Eppendorf tube with end-over-end mixing (Figure 3A). After removing the polymer-supported solid resin (containing bound *p*-nitrophenoxide ion) through pelleting (centrifugation) and microfiltration, FP **3u** (5 mM theoretical) remains in DMSO (Figure 3B). A concentration estimation can be performed by introducing a reference standard (e.g., tris(4-fluorophenyl) phosphine if the reaction is performed in [D_6]DMSO) to an aliquot of the newly generated FP **3** solution and measuring relative amounts by NMR (^1H, ^{31}P and/or ^{19}F). When using this calibration protocol for the reaction of **2u**→**3u** we determined that pure FP-rhodamine **3u** (3.75 mM) was ready for immediate screening as a [D_6]DMSO stock solution (see Figure 3C for an overview and Section 5.2 in the Supporting Information for details).

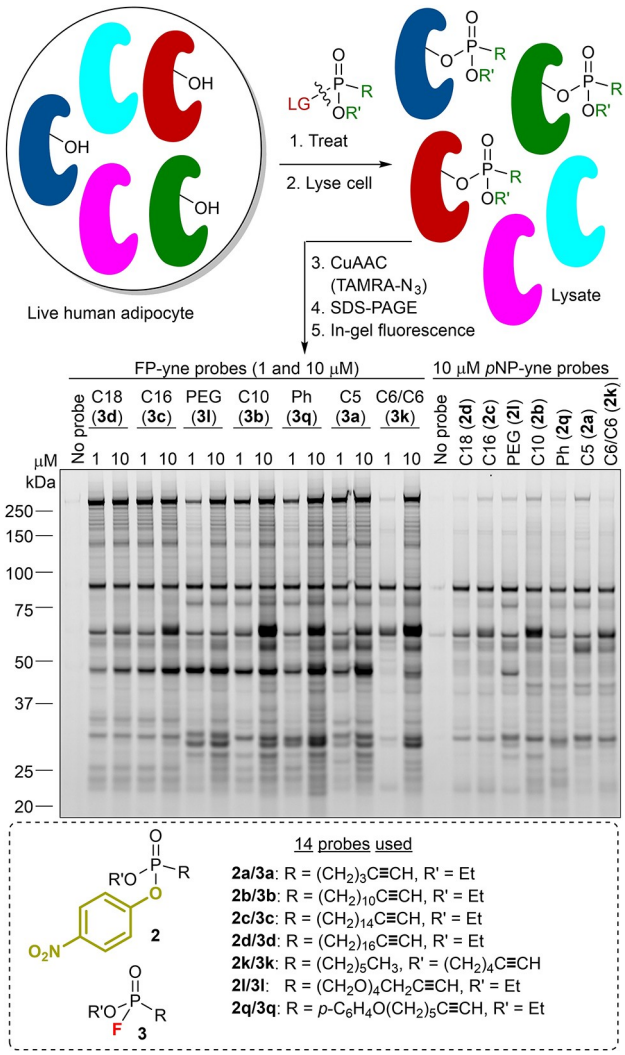

Figure 2. In-gel ABPP of phosphonate probes in human adipocytes.

We next compared the in-gel fluorescence intensity signals of a panel of 36 recombinant serine hydrolases of FP-rhodamine (**3u**) freshly prepared via our reaction-to-assay protocol versus those observed from historically generated data from **3u** prepared via traditional methods[6f] (Figure 3D1). Here, the loading control normalized intensities for each enzyme are plotted against each other. Linear regression of this dataset returned a slope of 1.01 and R^2 value of 0.99, an analysis that demonstrates the indistinguishability of the two batches. We compared the labeling profiles generated with these different samples of **3u** (FP-rhodamine) in competitive ABPP using this enzyme panel[22] and **3v** (FP-biotin) as broad-spectrum SH Inhibitor (see Section 5.3 in the Supporting Information for additional details). The pharmacological profile for this compound is shown as a heatmap in Figure 3D2, where the reagents again proved to be indistinguishable from each other with no notable discrepancies between the two results, further highlighting the robustness of our reaction-to-assay protocol.

In summary, we have demonstrated an effective strategy that uses *p*-nitrophenylphosphonates, not only as covalent inhibitors and activity-based probes of serine hydrolases, but also as stable, convenient, and broadly applicable late-stage synthetic precursors for the on-demand preparation of pure fluorophosphonates. The FP synthesis on-demand protocol was designed with operational simplicity and broad compatibility in mind, obviating many of the common issues previously associated with fluorophosphonate synthesis, isolation, and storage. The strategy facilitates and encourages pairwise comparisons of differentially reactive *p*-nitrophenylphosphonates and fluorophosphonates in activity-based profiling experiments, while also realizing additional efficiency and greater synergy between compound synthesis and screening, through simple adaptation of the new procedure into a reaction-to-assay format. We anticipate that this strategy and associated synthesis protocol will find broad

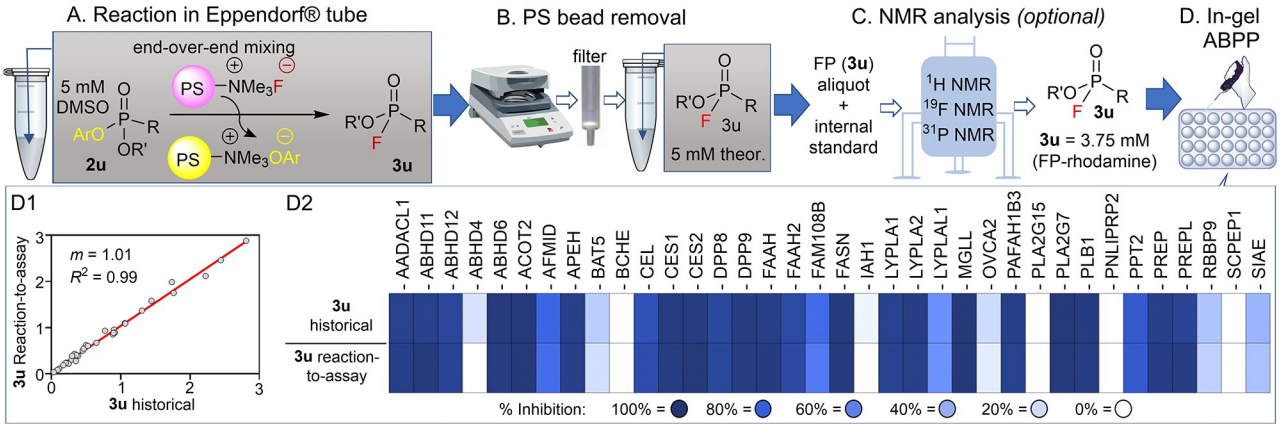

Figure 3. Reaction-to-assay workflow. A) Reaction setup. B) Removal of polymer-supported bead by pelleting and filtration yields pure FP stock solution in DMSO. C) Optional concentration determination by NMR analysis of the filtered FP stock solution aliquot against an internal standard. D1) Characterization of **3u** produced through the reaction-to-assay workflow. D2) In-gel ABPP labeling profiles of FP-biotin (**3v**) using different batches of FP-rhodamine (**3u**) with % inhibition data represented as a heatmap (see Section 5 in the Supporting Information for additional details).

application amongst those interested in profiling serine hydrolases with covalent phosphonate probes.

Experimental Section

All FP on-demand reactions were carried out in 1-dram septa-capped (PTFE-lined) vials and were equipped with micro stir bars. Commercially available fluoride on polymer support reagent (1.5–4.0 equiv)[23] was added to a solution of electron deficient mixed aryloxy phosphonate **2** (1 equiv) in CH_3CN (0.08–0.15 M). Note: the fluoride reagent bead color changes from light pink to bright yellow upon addition of mixed aryloxyphosphonates containing a *p*-nitrophenoxy leaving group. The reaction was stirred at room temperature until complete (75–330 min., determined by HPLC/MS and/or ^{31}P NMR). Stirring was ceased and the solution was removed from the solid-supported reagent carefully via pipette then filtered through a 0.2 μM nylon filter disc into a tared 1-dram vial. The reserved solid-supported resin was suspended in fresh CH_2Cl_2/CH_3CN (1.5 mL, 2:1 *v/v*), stirred at room temperature for 5 min, then filtered as above. The combined filtrates were concentrated under a light stream of nitrogen then dried under vacuum to afford pure fluorophosphonate **3**.

Acknowledgements

The authors gratefully thank and acknowledge Dongmei Li for providing us with differentiated human adipose-derived stem cells, Julie Keefer for assisting us with analytical HPLC/MS method development, and Doug Johnson for helpful suggestions.

Conflict of Interest

The authors declare no conflict of interests.

Keywords: activity-based protein profiling · aryl phosphonates · fluorophosphonates · serine hydrolases · solid-phase reagents · synthetic methods

[1] a) G. Dodson, A. Wlodawer, *Trends Biochem. Sci.* **1998**, *23*, 347–352; b) O. D. Ekici, M. Paetzel, R. E. Dalbey, *Protein Sci.* **2008**, *17*, 2023–2037; c) C. Powers, J. L. Asgian, O. D. Ekici, K. E. James, *Chem. Rev.* **2002**, *102*, 4639–4750.

[2] a) J. Z. Long, B. F. Cravatt, *Chem. Rev.* **2011**, *111*, 6022–6063; b) X. S. Puente, L. M. Sanchez, C. M. Overall, C. Lopez-Otin, *Nat. Rev. Genet.* **2003**, *4*, 544–558.

[3] D. A. Bachovchin, B. F. Cravatt, *Nat. Rev. Drug Discovery* **2012**, *11*, 52–68.

[4] a) D. S. Johnson, K. Ahn, S. Kesten, S. E. Lazerwith, Y. Song, M. Morris, L. Fay, T. Gregory, C. Stiff, J. B. Dunbar Jr., M. Liimatta, D. Beidler, S. Smith, T. K. Nomanbhoy, B. F. Cravatt, *Bioorg. Med. Chem. Lett.* **2009**, *19*, 2865–2869; b) E. Dominguez, A. Galmozzi, J. W. Chang, K. L. Hsu, J. Pawlak, W. Li, C. Godio, J. Thomas, D. Partida, S. Niessen, P. E. O'Brien, A. P. Russell, M. J. Watt, D. K. Nomura, B. F. Cravatt, E. Saez, *Nat. Chem. Biol.* **2014**, *10*, 113–121; c) D. Ogasawara, T. A. Ichu, V. F. Vartabedian, J. Benthuysen, H. Jing, A. Reed, O. A. Ulanovskaya, J. J. Hulce, A. Roberts, S. Brown, H. Rosen, J. R. Teijaro, B. F. Cravatt, *Nat. Chem. Biol.* **2018**, *14*, 1099–1108; d) J. S. Cisar, O. D. Weber, J. R. Clapper, J. L. Blankman, C. L. Henry, G. M. Simon, J. P. Alexander, T. K. Jones, R. A. B. Ezekowitz, G. P. O'Neill, C. A. Grice, *J. Med. Chem.* **2018**, *61*, 9062–9084.

[5] a) R. R. Rando, *Science* **1974**, *185*, 320–324; b) D. B. Lowe, S. Magnuson, N. Qi, A. M. Campbell, J. Cook, Z. Hong, M. Wang, M. Rodriguez, F. Achebe, H. Kluender, W. C. Wong, W. H. Bullock, A. I. Salhanick, T. Witman-Jones, M. E. Bowling, C. Keiper, K. B. Clairmont, *Bioorg. Med. Chem. Lett.* **2004**, *14*, 3155–3159; c) S. Hawthorne, R. Hamilton, B. J. Walker, B. Walker, *Anal. Biochem.* **2004**, *326*, 273–275; d) W. Li, J. L. Blankman, B. F. Cravatt, *J. Am. Chem. Soc.* **2007**, *129*, 9594–9595; e) U. R. Haedke, S. C. Frommel, F. Hansen, H. Hahne, B. Kuster, M. Bogyo, S. H. Verhelst, *ChemBioChem* **2014**, *15*, 1106–1110; f) A. F. Kornahrens, A. B. Cognetta III, D. M. Brody, M. L. Matthews, B. F. Cravatt, D. L. Boger, *J. Am. Chem. Soc.* **2017**, *139*, 7052–7061.

[6] a) Y. Liu, M. P. Patricelli, B. F. Cravatt, *Proc. Natl. Acad. Sci. USA* **1999**, *96*, 14694–14699; b) D. Kidd, Y. Liu, B. F. Cravatt, *Biochemistry* **2001**, *40*, 4005–4015; c) N. Jessani, Y. Liu, M. Humphrey, B. F. Cravatt, *Proc. Natl. Acad. Sci. USA* **2002**, *99*, 10335–10340; d) S. E. Tully, B. F. Cravatt, *J. Am. Chem. Soc.* **2010**, *132*, 3264–3265; e) B. R. Martin, C. Wang, A. Adibekian, S. E. Tully, B. F. Cravatt, *Nat. Methods* **2012**, *9*, 84–89; f) A. P. A. Janssen, D. van der Vliet, A. T. Bakker, M. Jiang, S. H. Grimm, G. Campiani, S. Butini, M. van der Stelt, *ACS Chem. Biol.* **2018**, *13*, 2406–2413; g) F. B. d'Andrea, C. A. Townsend, *Cell Chem. Biol.* **2019**, *26*, 878–884.

[7] a) M. L. Mannesse, J. W. Boots, R. Dijkman, A. J. Slotboom, H. T. van der Hijden, M. R. Egmond, H. M. Verheij, G. H. de Haas, *Biochim. Biophys. Acta.* **1995**, *1259*, 56–64; b) H. J. Deussen, S. Danielsen, J. Breinholt, T. V. Borchert, *Bioorg. Med. Chem. Lett.* **2000**, *10*, 2027–2031; c) H. Schmidinger, R. Birner-Gruenberger, G. Riesenhuber, R. Saf, H. Susani-Etzerodt, A. Hermetter, *ChemBioChem* **2005**, *6*, 1776–1781; d) S. Nickel, F. Kaschani, T. Colby, R. A. van der Hoorn, M. Kaiser, *Bioorg. Med. Chem.* **2012**, *20*, 601–606; e) M. Viertler, M. Schittmayer, R. Birner-Gruenberger, *Bioorg. Med. Chem.* **2012**, *20*, 628–632; f) S. Rengachari, P. Aschauer, M. Schittmayer, N. Mayer, K. Gruber, R. Breinbauer, R. Birner-Gruenberger, I. Dreveny, M. Oberer, *J. Biol. Chem.* **2013**, *288*, 31093–31104.

[8] a) S. Zweerink, V. Kallnik, S. Ninck, S. Nickel, J. Verheyen, M. Blum, A. Wagner, I. Feldmann, A. Sickmann, S. V. Albers, C. Brasen, F. Kaschani, B. Siebers, M. Kaiser, *Nat. Commun.* **2017**, *8*, 15352; b) C. Wang, D. Abegg, B. G. Dwyer, A. Adibekian, *ChemBioChem* **2019**, *20*, 2212–2216.

[9] F. Faucher, J. M. Bennett, M. Bogyo, S. Lovell, *Cell Chem. Biol.* **2020**, *27*, 937–952.

[10] a) J. L. Meier, A. C. Mercer, M. D. Burkart, *J. Am. Chem. Soc.* **2008**, *130*, 5443–5445; b) L. C. Gillet, K. Namoto, A. Ruchti, S. Hoving, D. Boesch, B. Inverardi, D. Mueller, M. Coulot, P. Schindler, P. Schweigler, A. Bernardi, S. Gil-Parrado, *Mol. Cell. Proteomics* **2008**, *7*, 1241–1253; c) X. Wang, T. Guo, J. Chen, X. Li, Y. Zhou, Z. Pan, *Chem. Commun.* **2018**, *54*, 4661–4664.

[11] P. A. Messina, K. C. Mange, W. J. Middleton, *J. Fluorine Chem.* **1989**, *42*, 137–143.

[12] a) F. Ishikawa, T. Tsumuraya, I. Fujii, *J. Am. Chem. Soc.* **2009**, *131*, 456–457; b) B. Wieczorek, B. Lemcke, H. P. Dijkstra, M. R. Egmond, R. J. M. Klein Gebbink, G. van Koten, *Eur. J. Inorg. Chem.* **2010**, *2010*, 1929–1938.

[13] H. Susani-Etzerodt, H. Schmidinger, G. Riesenhuber, R. Birner-Gruenberger, A. Hermetter, *Chem. Phys. Lipids* **2006**, *144*, 60–68.

[14] a) H. P. Dijkstra, H. Sprong, B. N. Aerts, C. A. Kruithof, M. R. Egmond, R. J. Klein Gebbink, *Org. Biomol. Chem.* **2008**, *6*, 523–531; b) B. Wieczorek, A. Träff, P. Krumlinde, H. P. Dijkstra, M. R. Egmond, G. v Koten, J.-E. Bäckvall, R. J. M. K. Gebbink, *Tetrahedron Lett.* **2011**, *52*, 1601–1604.

[15] S. D. Field, W. Lee, J. K. Dutra, F. S. F. Serneo, J. Oyer, H. Xu, D. S. Johnson, C. W. am Ende, U. Seneviratne, *ChemBioChem* **2020**, *21*, 2916–2920.

[16] a) G. T. Davis, M. M. Demek, J. R. Sowa, J. Epstein, *J. Am. Chem. Soc.* **1971**, *93*, 4093–4103; b) K. K. Ogilvie, S. L. Beaucage, N. Theriault, D. W. Entwistle, *J. Am. Chem. Soc.* **1977**, *99*, 1277–1278; c) Y. S. Simanenko, A. F. Popov, T. M. Prokop'eva, E. A. Karpichev, V. A. Savelova, I. P. Suprun, C. A. Bunton, *Russ. J. Org. Chem.* **2002**, *38*, 1286–1298; d) C. Lapeyre, M. Delomenede, F. Bedos-Belval, H. Duran, A. Negre-Salvayre, M. Baltas, *J. Med. Chem.* **2005**, *48*, 8115–8124; e) M. Delomenede, F. Bedos-Belval, H. Duran, C. Vindis, M. Baltas, A. Negre-Salvayre, *J. Med. Chem.* **2008**, *51*, 3171–3181; f) S. Kaleem Ahmed, Y. Belabassi, L. Sankaranarayanan, C. K. Chao, J. M. Gerdes, C. M. Thompson, *Bioorg. Med. Chem. Lett.* **2013**, *23*, 2048–2051; g) A. W. Tuin, M. A. Mol, R. M. van den Berg, A. Fidder, G. A. van der Marel, H. S. Overkleeft, D. Noort, *Chem. Res. Toxicol.* **2009**, *22*, 683–689.

[17] T. J. de Boer, H. J. Backer, *Org. Synth.* **1956**, *36*, 16.

[18] a) H. Huang, J. Denne, C. H. Yang, H. Wang, J. Y. Kang, *Angew. Chem. Int. Ed.* **2018**, *57*, 6624–6628; *Angew. Chem.* **2018**, *130*, 6734–6738; b) P. Adler, A. Pons, J. Li, J. Heider, B. R. Brutiu, N. Maulide, *Angew. Chem. Int. Ed.* **2018**, *57*, 13330–13334.

[19] M. Fananas-Mastral, B. L. Feringa, *J. Am. Chem. Soc.* **2014**, *136*, 9894–9897.
[20] a) G. Cainelli, F. Manescalchi, M. Panunzio, *Synthesis* **1976**, *1976*, 472–473; b) B. Hinzen, M. G. Hahn in *Combinatorial Chemistry: From Theory to Application, Vol. 26* (Eds.: W. Bannwarth, B. Hinze), Wiley-VCH, Weinheim, **2006**, pp. 457–512.
[21] J. W. Chang, A. B. Cognetta, 3rd, M. J. Niphakis, B. F. Cravatt, *ACS Chem. Biol.* **2013**, *8*, 1590–1599.
[22] L. A. McAllister, C. R. Butler, S. Mente, S. V. O'Neil, K. R. Fonseca, J. R. Piro, J. A. Cianfrogna, T. L. Foley, A. M. Gilbert, A. R. Harris, C. J. Helal, D. S. Johnson, J. I. Montgomery, D. M. Nason, S. Noell, J. Pandit, B. N. Rogers, T. A. Samad, C. L. Shaffer, R. G. da Silva, D. P. Uccello, D. Webb, M. A. Brodney, *J. Med. Chem.* **2018**, *61*, 3008–3026.
[23] Fluoride on polymer support reagent. CAS no. 39339–85-0. Commercially available from Sigma–Aldrich (catalog no. 387789). Stoichiometry was calculated based on the lower limit (2.0 mmol g of the load factor range (2.0–3.0 mmol g reported by the reagent manufacturer.

Manuscript received: December 16, 2020
Revised manuscript received: January 23, 2021
Accepted manuscript online: January 24, 2021
Version of record online: ■■, ■■■

COMMUNICATIONS

Not too demanding: A robust and purification-free, one-step synthesis has been developed to enable the on-demand preparation of structurally diverse fluorophosphonates from a stable, and storable "toolbox" of readily accessible *p*-nitrophenyl-phosphonates. Additionally, a reaction-to-assay protocol is highlighted that further facilitates the rapid screening of these valuable activity-based probes.

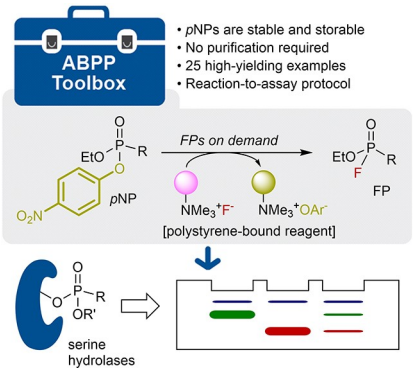

J. K. Dutra, Dr. T. L. Foley, Dr. Z. Huang, Dr. E. L. Fisher, E. A. Lachapelle, Dr. S. Mahapatra, K. Ogilvie, T. W. Butler, J. Bellenger, Dr. J. Devraj Majmudar, Dr. C. W. am Ende*